Design and synthesis of transparent and flexible nanofibrillated cellulose films to replace petroleum-based polymers

Mariem Lassoued,[a] Frank Crispino,[b] Eric Loranger[a*]

[a]I2E3 – Institut d'Innovations en Écomatériaux, Écoproduits et Écoénergies à base de biomasse, Université du Québec à Trois-Rivières Trois-Rivières, QC, G9A 5H7, Canada

[b] Laboratoire de recherche en criminalistique, Université du Québec à Trois-Rivières Trois-Rivières, QC, G9A 5H7, Canada

Mariem Lassoued

E-mail: Mariem.Lassoued@uqtr.ca

Tel: (+1) 819 376-5011, Ext 4518

Frank Crispino

E-mail: Frank.Crispino@uqtr.ca

Tel: (+1) 819 376-5011, Ext 3845

Eric Loranger* (Corresponding author)

E-mail : Eric.loranger1@uqtr.ca

Tel: (+1) 819 376-5011, Ext 4518

Abstract

Nanofibrillated cellulose films have garnered attention due to their interesting proprieties such as transparency and high mechanical strength. However, they are brittle, very hydrophilic, which is decreasing their potential applications. We have successfully achieved a simple and effective chemical modification based on polymer grafting and through plasticizer additions to increase the performance of the films as well as to improve the compatibility within conventional polymer. A preliminary study shows the possibility of using this film as an interlayer in safety glazing and/or bulletproof glass with polyvinyl butyral (PVB). The modified NFC films displays high optical transmittance (93%), increases tensile stretch and is more hydrophobic (83°). A higher flexibility was also achieved, as the film was greatly stretched and bended without cracking or breaking. The

NFC / PVB composite has three times more elongation at break, 13% more specific energy absorbed with a half-tensile stress compared to an interlayer of PVB.

1. Introduction

In recent decades, petroleum-based plastics have emerged and diversified to reach a considerable space in our daily life due to their numerous advantages, which allow to adapt to the desired applications. According to a study by the University of Santa Barbara in California in 2017, global production of plastics reached 9.1 billion tonnes, more than half of this volume, 5.4 billion tonnes, has ended in the environment (Simon & Schulte, 2017). However, in addition to the sustainability problems arising from the depletion of fossil fuels, the environmental impacts due to the wide use of these non-renewable sustainable materials are seriously increasing, putting terrestrial and aquatic ecosystems at risk (Bagheri, Radi, & Amiri, 2019; Floyd, 2016; Kumar Singla, Maiti, & Ghosh, 2016; Simon & Schulte, 2017). Therefore, a rational use of biodegradable polymers derived from renewable resources combined with an improvement in the quantity and quality of recycling, are the key points of sustainable development of plastics materials (Floyd, 2016). Nevertheless, the research on bio-based plastics produced from cellulose derivatives is challenging because of the complexity in recycling strategies and far from providing a long-term sustainable solution (Bagheri et al., 2019; Kumar Singla et al., 2016).

The 4-acetamido-2, 2, 6, 6 tetramethylpiperidine-1-oxyl (TEMPO) oxidized cellulosic nanofibrils, NFC, are promising nanomaterials, widely used as attractive biopolymers for the production of biobased films. The obtained films received reasonable attention because of their large specific surfaces, rigidity, transparent nature and biodegradability (Bideau, Cherpozat, Loranger, & Daneault, 2016; García, Gandini, Labidi, Belgacem, & Bras, 2016; Islam & Rahman, 2019; Niu, Gao, & Wu, 2014; Rol, Belgacem, Gandini, & Bras, 2019; Syverud, Xhanari, Chinga-Carrasco, Yu, & Stenius, 2011; Xhanari, Syverud, Chinga-Carrasco, Paso, & Stenius, 2011). However, the non-flexibility and hydrophilic nature limits their potential applications in many fields and affects their compatibility in most non-polar polymer matrices. Therefore, modifications of the surface chemistry of NFCs were used in order to improve the performance of the films as well as their compatibility with the polymer matrix (Islam & Rahman, 2019; Rol et al., 2019; Syverud et al., 2011; Xhanari et al., 2011). The major challenge of modifying NFC is to increase the

hydrophobicity and flexibility of the films while keeping satisfactory mechanical and optical properties (Tong, Chen, Tian, & He, 2020). The originality of our work is to synthesize flexible, transparent and less hydrophilic nanofibrillated cellulose (NFC) films, but in a purely aqueous medium.

In our study, NFC is chemically modified by radical polymerization of glycidyl methacrylate (GMA) in aqueous medium. The monomer GMA, which is inexpensive and highly reactive (Kocak, Solmaz, Tuncer, & Bütün, 2019), is often used to improve the mechanical properties and hydrophobicity of films including cellulose-based films. It is also used as a compatibilizer and coupling agent in the manufacture of composites (Abbasi et al., 2018; Cherifi, Boukoussa, Zaoui, Belbachir, & Meghabar, 2018; Faria et al., 2019; Khan et al., 2018; Kocak et al., 2019; Reis et al., 2009). Other studies have shown that adding plasticizers can improve the flexibility of films such as, starch–chitosan films (Liu, Adhikari, Guo, & Adhikari, 2013), Na-alginate films (Bagheri et al., 2019), silk fibroin films (Li et al., 2018), corn starch films (Šoltýs et al., 2019) and cellulose acetate oleate films (Tedeschi et al., 2018). Glycerol is generally recognized as one of the most suitable plasticizers (Bagheri et al., 2019; Li et al., 2018; Liu et al., 2013; Šoltýs et al., 2019).

The objective of the current research is to synthesize transparent and biodegradable films, which would have satisfactory mechanical properties like resistance and elongation at break, and an improvement of hydrophobic character compared to pure NFC film. Therefore, a simultaneous modification of NFC oxidized TEMPO by GMA and glycerol was performed. According to the literature, the amounts of monomer and plasticizer can significantly influence the characteristics of films (Abbasi et al., 2018; Bagheri et al., 2019; Pracella, Haque, Paci, & Alvarez, 2016). Therefore, a statistical response surface model was developed to study changes in the target properties of the final product. This method has been widely used to optimize the process conditions using a mathematical algorithm based on experimental results generated from experiments designed by statistical analysis software. Response-surface design overcomes the drawbacks of traditional optimization methods, which monitor the effect of a single parameter on the process at a time regardless of the interactive effects among the parameters examined. In addition, using statistical analysis requires less time and chemicals compared to the optimization of each parameter separately.

2. Experimentation

2.1. Materials

The pulp used in this work is a bleached kraft pulp of resinous wood from the paper company Domtar. The catalyst 4-acetamido-TEMPO is purchased from Sigma-Aldrich (Canada) and the sodium bromide from Fisher Scientific (Canada). The sodium hypochlorite used is 6 % concentrated as found in supermarkets. Poly (vinyl butyral-co-vinyl, alcohol-co-vinyl acetate) powder (Co PVB,>90 %, Sigma), glycidyl methacrylate (GMA, 97%, Sigma) and glycerol (99%, Sigma) are used as received. The other chemicals and solvents are laboratory grade and supplied by Sigma-Aldrich (USA) without further purification.

2.2. Preparation of NFC by TEMPO-mediated oxidation

The preparation of TEMPO oxidized NFCs is carried out based on a previously published protocol from our research group (Loranger, Paquin, Daneault, & Chabot, 2011; Paquin, Loranger, Hannaux, Chabot, & Daneault, 2013; Rattaz, Mishra, Chabot, & Daneault, 2011). The basic principle consists in the oxidation of cellulose fibers by adding NaClO to aqueous cellulose suspensions in the presence of catalytic amounts of 2, 2, 6, 6-tetramethyl-1-piperidinyloxy (TEMPO) and NaBr at pH 10–11 at room temperature. Ultrasounds are optional and may be used to further reduce the amounts of reactive used without any effect on the final properties of the nanofibrillated cellulose. The NFCs obtained had a carboxyl content of 1700 mmol / kg. The obtained NFC gel is dispersed in a homogenizer as optimized by Loranger et al. (Loranger, Piché, & Daneault, 2012).

2.3. Preparation of modified NFC film

The TEMPO oxidized NFC gel (3.3%) is diluted 50% up to 1.65 % with distilled water and then centrifuged for 15 minutes at 13,000 rpm. A transparent aqueous dispersion is obtained (0.1%) by recovering the supernatant and removing the micro suspensions. Then, the aqueous NFC solution is concentrated up to 0.9% using a rotavapor.

The modification consists in synthesizing poly (glycidyl methacrylate)-co-NFC (PGMA-co-NFC) followed by the addition of a plasticizer. An aqueous solution of NFC (200 ml) is stirred magnetically with ammonium persulfate (APS) (0.05 ± 0.0001 g) to initiate the in situ

polymerization of GMA. Then different volumes of glycidyl methacrylate (GMA) are added at 40°C. After stirring for 48 hours, different amounts of glycerol as a plasticizer are added at 70°C for 5 hours. Based on a Response-surface design as explained earlier, Table 1 shows the composition of the mixtures prepared in this study. Finally, the solutions are poured into aluminum cups and dried in an oven at 30°C for 2 days.

2.4. Preparation of composite NFC/PVB

The PVB / NFC composite is prepared by a coating method developed by our group (Maury, Loranger, & Daneault, 2016). First, the PVB is mixed with anhydrous ethanol (1% by weight) and stirred for 30 minutes until being completely dissolved. Then, the solution is poured into an aluminum cup already containing a previously dried NFC film. Finally, the cup is dried in an oven at 30°C for 2 days.

2.5. Characterization

Fourier-transform infrared spectroscopy (FTIR). The functional groups of native and modified NFC are analyzed by infrared spectroscopy FTIR in the range of 4500–600 cm^{-1} from 16 scans with a resolution of 4 cm^{-1}. FT-IR Spectra are obtained using a Nicolet™ IS10 FT-IR™ spectrometer (ThermoScientific™, USA) at room temperature.

Mechanical properties. The mechanical properties of the films are measured by universal testing machine Instron 4201™ equipped with a 500 N load cell. Rectangular shaped samples (30 mm length, 15 mm width) are stretched at a rate of 10 mm min^{-1}. All the stress-strain curves are recorded in a controlled room at 25°C and a relative humidity (RH) of 50%. Three measurements are carried out for each sample. As the mean and median values are very close, only the mean is reported. The Young's modulus, the stress, the elongation at break and the absorbed energy values are extracted from the stress-strain curves. A specific energy absorbed is calculated by the ratio between the energy absorbed at automatic break and the cross area of the sample. The thicknesses are measured with a Lhomargy™ micrometre (± 0.01 mm).

Transparency. Light transmission of films is measured by a Tint Meter Inspector Model 200™.

Scanning electron microscopy (SEM). Scanning electron micrographs of the cross-section and surfaces of the samples are obtained by scanning electron microscopy (SEM) with a JEOL JSM T300™ microscope. An acceleration voltage of 5 KV and magnification of 2500× (cross section)

and 1000× (surface) are used to observe the morphology of samples. Before analysis, all samples are deposited on a steel plate and coated with a mix of gold and platinum.

Contact angle. In order to characterize the hydrophobicity of the film surface, a FTA4000™ contact angle measuring system (First Ten Angstroms) is used. Water contact angles are measured with the drop method at room temperature at five different locations on each surface. One drop (0.8 µl ± 0.07) of purified water (milli Q) is deposited on the surfaces and 300 images are captured within 90 s.

Thermogravimetric Analysis (TGA). Analysis of the thermal stability of the samples is carried out in a Perkin-Elmer™ Thermogravimetric analyzer TGA 8000™ (Pyris Series). The samples (Table1) are heated in platinum pans from 50 to 575°C, under a nitrogen atmosphere, at a heating rate of 5°C / min. Then the samples are heated from 575 to 900°C of 10°C / min under a nitrogen flow of 20 ml / min.

Statistical analysis. To assess the effect of the amounts of monomer (GMA) and plasticizer (glycerol) on the properties of the film, a central composite design-response surface model (CCD) is used. Preliminary results in the laboratory showed that for an amount of 200 ml of NFC, if the volumes of GMA and glycerol are increased to more than 4.5 and 1 ml respectively, no film can be obtained. Therefore, a volume of GMA in the range of 0 to 4.5 ml and a volume of glycerol in the range of 0 to 1 ml were introduced to the JMP® Start Statistics 2007 (SAS Institute Inc.™, Cary, NC, USA) to design the experiments (Table1). Consequently, 11 different random experimental combinations of variables including 3 central points were proposed and their corresponding responses were measured.

Table 1. *Response-Surface design array of experiments*

Test number	Sample name	Volume of GMA (ml)	Volume of Plasticizer (ml)
1	NFC 1	2.25	1
2	NFC 2	2.25	0.5
3	NFC 3	4.5	0
4	NFC 4	4.5	0.5
5	NFC 5	4.5	1
6	NFC 6	2.25	0.5
7	NFC 7	2.25	0
8	NFC 8	0	1
9	NFC 9	2.25	0.5
10	NFC 10	0	0.5
11	NFC 11	0	0

3. Results

3.1. Fourier-transform infrared spectroscopy (FTIR)

The FTIR spectra (600-4000 cm^{-1}) of pure NFC 11, modified NFC 3 films are shown in Figure 1. The analysis of the spectra shows that the chemical structure of the NFC does not change during the modification process, as characteristic bands typical of the original form were observed. The band located at 3404 cm^{-1} is attributed to OH stretching vibrations, the band at 2904 cm^{-1} to CH_2 stretching vibrations and the band at 1660 cm^{-1} to carboxylic functional groups of native NFC film. The band at 1720 cm^{-1} and the weak broad band at 1285 cm^{-1} are attributed to the C=O and C-O stretching of GMA, respectively (Abbasi et al., 2018; Faria et al., 2019). The schematic of modifying the cellulose to obtain a modified NFC film is shown in Figure 2A while photographs of NFC 4 films are found in Figure 2B for comparison purposes.

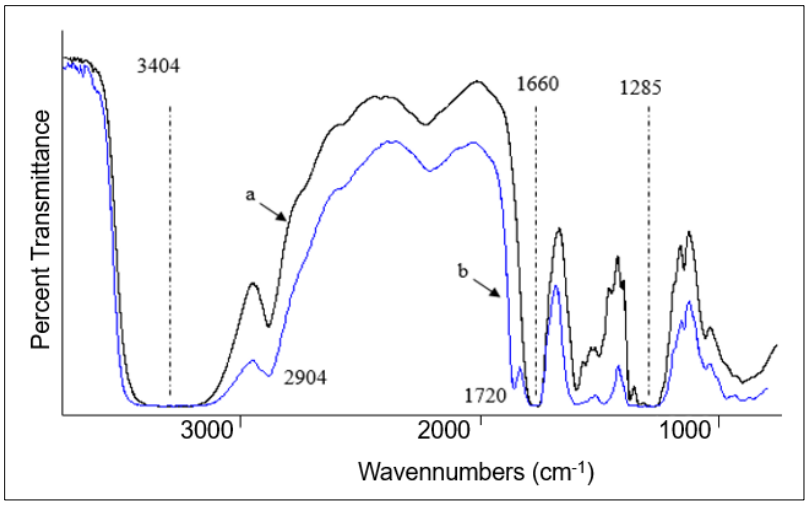

Figure 1. *ATR-FTIR spectra of pure NFC 11 (a), modified NFC 3 (b) films*

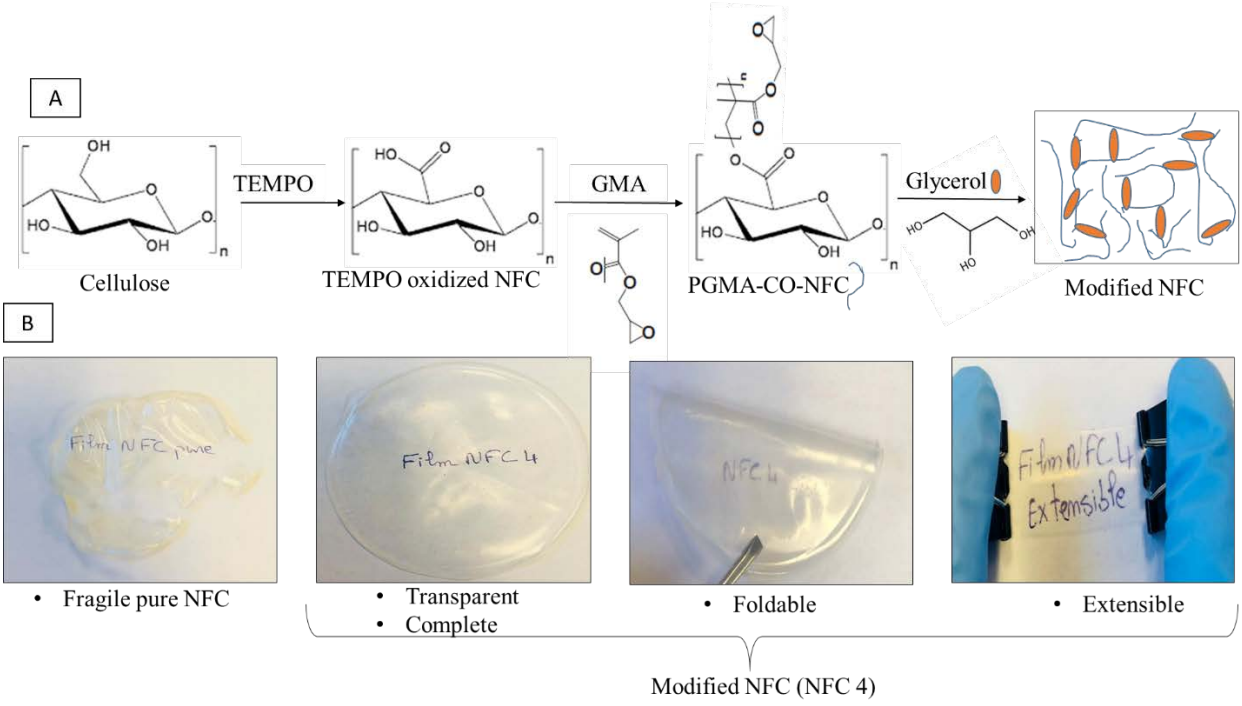

Figure 2.A) Schematic of cellulose modifications, B) Photographs of the pure NFC and modified NFC (Example: NFC 4) films placed on a white background paper to demonstrate their properties

3.2. Effect of monomer and plasticizer quantities

A central composite design-response surface model is applied for modeling and optimizing the influence of GMA quantity (X1) and glycerol quantity (X2) on the properties of the films: Young's

205 modulus E (Y1), tensile stress (Y2), elongation at break ε (Y3), specific absorbed Energy (Y4),
206 contact angle (Y5) and light transmission (Y6). Results from experiments are illustrated in Table
207 2. Analysis of variance is used to identify the significance of factors with a P value < 0.05. Based
208 on the regression coefficient (R^2) and adjusted regression coefficient ($adjR^2$), polynomial models
209 for each response are determined. Thus, the execution of the model provides Iso-response profilers,
210 which help determine the variation of responses for each combination of factors (Figure 3).
211 Table 2. *Experimental design and results of different dependent variables*

Test number	**X1 (ml)**	**X2 (ml)**	**Y1 (MPa)**	**Y2 (MPa)**	**Y3 (%)**	**Y4 (J/cm^2)**	**Y5 (°)**	**Y6 (%)**
1	2.25	1.0	32.0	1.2	5.1	0.1	83.0	93.0
2	2.25	0.50	67.9	4.6	13.7	1.0	46.3	73.0
3	4.50	0.00	1016.0	7.5	1.3	0.1	51.8	70.0
4	4.50	0.50	156.4	8.1	13.2	2.5	76.6	90.0
5	4.50	1.00	22.0	3.3	16.4	0.9	81.7	93.0
6	2.25	0.50	79.3	5.1	16.1	1.8	50.1	75.0
7	2.25	0.00	2324.8	11.6	1.6	0.2	52.3	34.0
8	0.00	1.00	23.7	0.9	12.3	0.3	37.8	93.0
9	2.25	0.50	66.4	4.8	17.9	1.6	43.2	74.0
10	0.00	0.50	47.4	2.6	12.5	0.7	34.7	85.0
11	0.00	0.00	2168.7	16.5	2.2	0.3	38.3	93.0

212

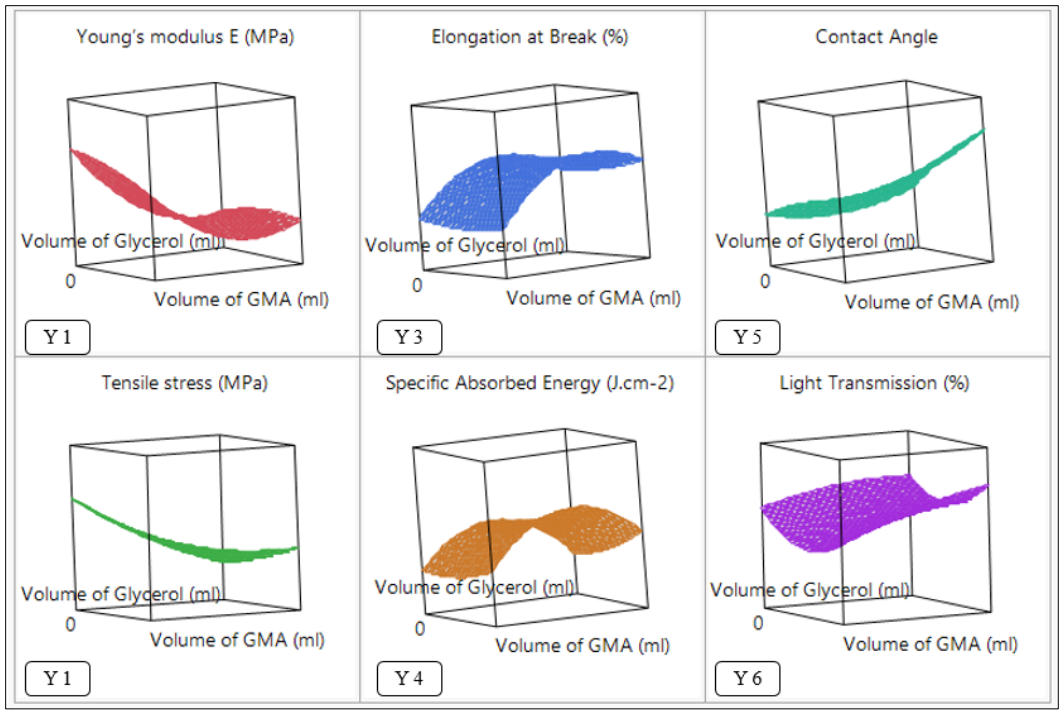

Figure 3. *Iso-response profilers predicting effects of GMA (horizontal axis) and glycerol (vertical axis) volumes on Young's modulus E (Y1), tensile stress (Y2), Elongation at break ε (Y3), Specific Absorbed Energy (Y4), Contact Angle (Y5) and Light Transmission (Y6)*

3.2.1. Mechanical properties

Tensile stress-strain curves of pure NFC 11, modified NFC 3, 4, 5 and 6, Films are shown in Figure 4. Pure NFC film (NFC 11) is a fragile material, which fractures directly when it is subjected to mechanical stress. Previous research has shown that the rupture of brittle materials is due to the presence of initial defects (Hild, 1992). This is confirmed by the shape of the stress-strain curve. The detection of breaking point for this type of material is very difficult so, we had to stop the testing manually.

The modification of NFC increases the elongation at break to around 17.9 % (Film 9) to be compared with an elongation at break of 2.2% for pure NFC film. Contrariwise, the tensile strain values of the purest natural polymer-based film are around 15% (Huang, Zhong, Zhang & Cai, 2017; Tong, Chen, Tian, & He, 2020). NFC films modified by GMA and glycerol simultaneously exhibit ductile behavior, which undergoes great deformation before rupture. The photographs shown in Figure 2 confirm these results. The modified film (Example film 4) can be rolled, folded

and stretched without cracking. These advantages can lead to a much-improved NFC-based film for applications that require transparent and flexible films.

The results from the statistical analysis show that the change in the volume of glycerol has a significant effect on the mechanical properties of the film while the amount of GMA has no. As shown in Figure 3, when the glycerol volume increases, the Young's modulus E and tensile stress decrease, however, the elongation at break ε and absorbed energy increase. This is explained by the plasticizing effect of the glycerol (Li et al., 2018; Liu et al., 2013). Therefore, a minimum level of glycerol volume is determined to achieve maximum rigidity, whereas a maximum level is determined as optimum to achieve maximum flexibility. These results are confirmed by tensile stress-strain curves presented on Figure 4. Indeed, for a same volume of GMA (4.5 ml), when the quantity of glycerol increases from 0.25, 0.5 to 1 ml, we can clearly see the change in the shape of the curves towards a more ductile behavior of NFC 3, 4, 5 films respectively. The model equations are:

$$\mathrm{Y1}\left(\text{Young's modulus E (MPa)}\right) = 83.492 - 905.308\mathrm{X2} + 847.696\mathrm{X2}$$
$$(\mathrm{R}^2 = 87\%\,, \mathrm{R}^2\mathrm{adj} = 84\%)$$
$$\mathrm{Y2}\left(\text{Tensile stress (MPa)}\right) = 6{,}011 - 5{,}057\mathrm{X2}$$
$$(\mathrm{R}^2 = 69\%,\ \mathrm{R}^2\mathrm{adj} = 66\%)$$
$$\mathrm{Y3}\left(\text{Elongation at break } \varepsilon\ (\%)\right) = \ 14{,}683 + 4{,}778\mathrm{X2} - 8{,}175\mathrm{X2}^2$$
$$(\mathrm{R}^2 = 79\%, \mathrm{R}^2\mathrm{adj} = 74\%)$$
$$\mathrm{Y4}\ (\text{Specific Absorbed Energy } (\mathrm{J.cm^{-2}})) = \ 1{,}524 + 0{,}127\mathrm{X2} - 1{,}206\mathrm{X22}$$
$$(\mathrm{R}^2 = 64\%, \mathrm{R}^2\mathrm{adj} = 55\%)$$

Even though the statistical analysis shows no significant effect on addition of GMA, visual tests support that this step is very important to obtain a complete NFC films, maintaining similar mechanical properties of pure NFC films, which are fragile and crack down easily while handling (Figure 2). This is particularly the case when comparing NFC 11 to NFC modified with GMA only NFC 3. In addition, tensile stress-strain curves of NFC 6 and 4 films (Figure 4) show that, for the same amount of glycerol (0.5 ml), when we increase the quantity of the monomer (GMA) from 2.25 to 4.5 ml respectively, tensile stress increases, while tensile strain decreases.

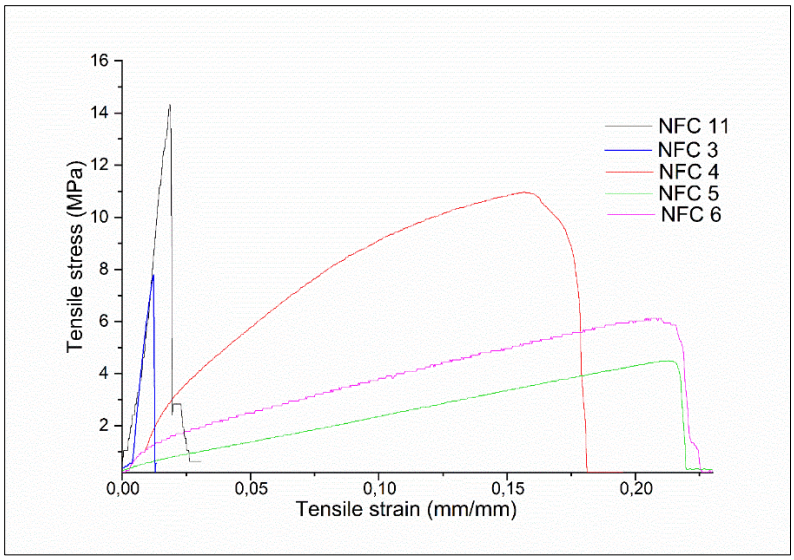

Figure 4. Tensile stress-strain curves of pure NFC 11, modified NFC 3, 4, 5 and 6, Films

3.2.2. Contact angle measurements

It is clear from the Table 1 and Iso-response profilers (Figure 3) that both glycerol and GMA volumes have significant effects on contact angle which is increased from 38.3° (pure film 11) to 83° (modified film 1). To support our results, Figure 5 shows the droplet profiles and the evaluation of the contact angle on different types of films: pure NFC (NFC 11), NFC modified with only GMA (Example NFC 3), NFC modified with only glycerol (Example NFC 8) and NFC modified with both GMA and glycerol respectively. Previous studies have shown that the grafting of epoxy chains onto allyl cellulose increases the hydrophobicity of the films (Tong, Chen, Tian, & He, 2020). These observations are confirmed by our study, for films 3 (51.8°) and films 7 (52.3°). On the other hand, the addition of only glycerol has an opposite effect and the contact angle of the films always remains small, e.g. film 8 (37.8°) and film 10 (34.7°). These results are also confirmed by previous studies (Coupland, Shaw, Monahan, O'Riordan, & O'Sullivan). However, the contact angle results drawn from this study show that the polymerization by GMA followed by the addition of plasticizer presents an excellent compromise for increasing the hydrophobic character of the films as shown by film 1 (83°), film 4 (76.6°) and film 5 (81.7°) (Figure 5). The outstanding flexible and transparent cellulose films show contact angle values higher than that of nanocellulose film (47°) (Fukuzumi, Saito, Iwata, Kumamoto, & Isogai, 2009) and modified nanocellulose film, of which contact angle does not exceed 79° (Tong, Chen, Tian, & He, 2020). Ultimately, the model equation for Contact Angle Y5 is given by:

$$Y5\ (\text{Contact Angle}\ ) = 54{,}173 + 16{,}555X1 + 10{,}029X2 + 7{,}595X1X2$$

$$(R^2 = 77\%, R^2adj = 68\%)$$

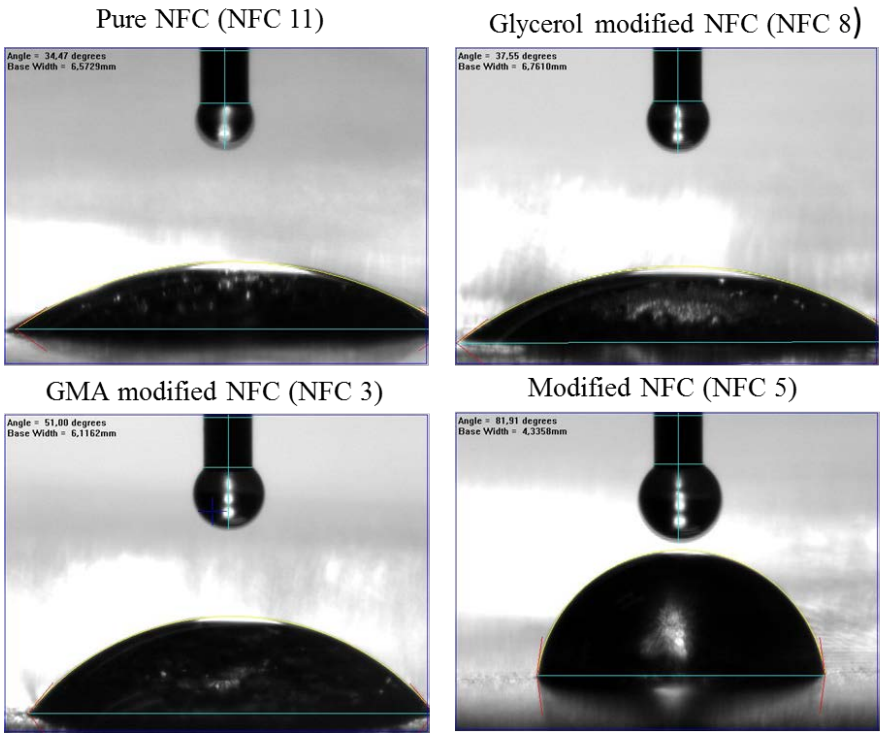

Figure 5.Water contact angles of pure NFC 11, Glycerol modified NFC (NFC 8), GMA modified NFC (NFC 3) and modified NFC (NFC 5)

3.2.3. Optical properties

The optical transmittance values of our films are very promising. Hence, the majority of the films obtained (Table 2) show high light transmittance values (optimal 93%) (Figure 2). They are comparable to those of commercial cellophane (85%), Nanopaper (90%) (Tong, Chen, Tian, & He, 2020) and ginger nanofiber (82%) (Abral et al., 2020) films. However, the film NFC 3 (70%) and film NFC 7 (34%) have moderately to low light transmission values. Statistical analyses with p value < 0.05 do not indicate which factor has a significant effect on the optical transmittance of films. Nevertheless, based on Iso-response profilers (Figure 3) we can notice that the presence of glycerol increases the transparency of the films. In fact, studies have shown that the glycerol plasticizer improves the homogeneous dispersion in the polymer matrix by interfacial interactions (Figure 2 (A)) (Li et al., 2018).

3.3. Morphological characterization

Figure 6 shows the comparison of SEM micrographs of the cross section and surfaces of pure NFC and modified NFC with both GMA and glycerol. The surface morphology of the modified NFC is more homogeneous and clearly different, supporting successful modification of TEMPO oxidized NFC. As it has been demonstrated by Liu et al. (Liu, Adhikari, Guo, & Adhikari, 2013), the formation of plasticized and rubbery films is supported by the formation of a homogeneous and smooth surface. The cross-section micrographs show that the pure NFC appears as a layer with a few pores and cracks whereas the modified NFC seems to be strongly entangled and less porous showing that probably more interactions between modified NFC. In conclusion, SEM images show a strong entanglement of the multiple layers of NFC.

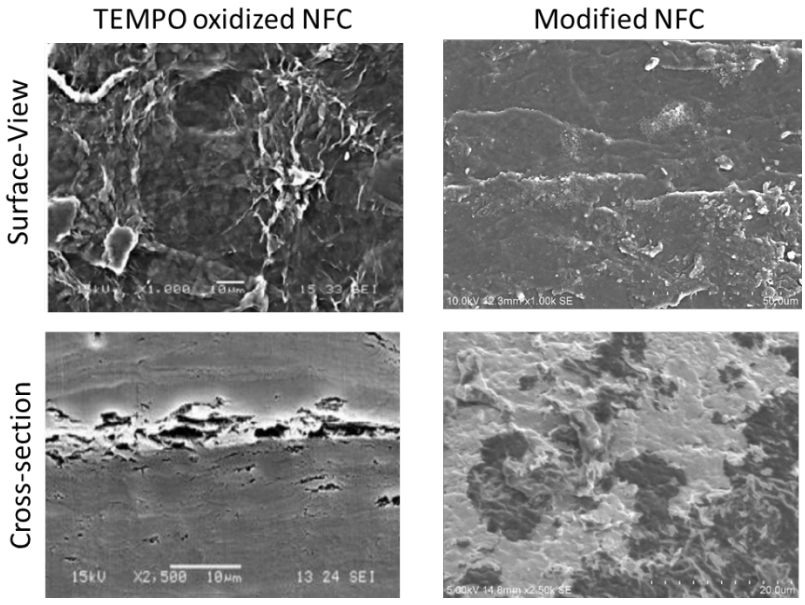

Figure 6. SEM micrographs of the cross section and surfaces of pure NFC and modified NFC

3.4. Thermogravimetric Analysis

Thermal behaviours of NFC based-films are studied using Thermogravimetric analysis (TG) under nitrogen atmosphere from 50-900°C (Figure 7). In all the curves, the first part of the analysis from

50 to 105 ° C was removed because it corresponds to the evaporation of solvent (water). Thus, depending on the water content, the curves may not start at 100% in weight. Initially, the modified films (NFC 2, 3) show a thermal stability from 50 up to 200°C more than the native film (NFC 11). The first decrease in the mass of pure NFC 11 film shows up to 140° C, which could be attributed to the release of moisture and a weakly bonded water, while the modified films show a lower weight loss due to its more hydrophobic characteristics (Ashori, Babaee, Jonoobi, & Hamzeh, 2014). In addition, the modification of NFC by grafting only PGMA (NFC 3) was found to introduce thermal degradation behavior in several stages. The first and second decomposition steps (240.07°C and 384.03°C) can be attributed to the decomposition of the glycidyl and carboxyl groups of the GMA respectively (Abbasi et al., 2018; Cherifi et al., 2018). For the modification by grafting of PGMA followed by the addition of plasticizer (NFC 2-6-9), we note the appearance of a new degradation step at 172.98°C, which can be attributed to the decomposition of glycerol. As shown in Figure 7, the proposed modification of NFC has increased the thermal degradation resistance of the films at higher temperature.

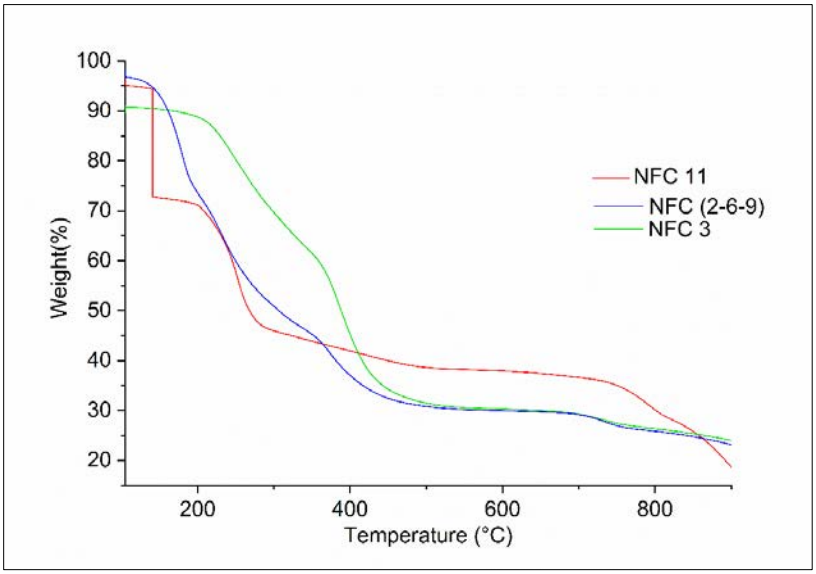

Figure 7. Thermogravimetric analysis of pure NFC 11, NFC (2-6-9) and NFC 3 films

3.5. Discussion: NFC/PVB composite

Today, safety glass is laminated using a thermoplastic polymer, polyvinyl butyral (PVB) which is petroleum-made, non-biodegradable and expensive. NFC 4 film was chosen to synthesize a NFC / PVB composite as a candidate interlayer for safety glass and bulletproof glazing because of its

interesting properties such as flexibility, transparency and above all, the highest specific absorbed energy (2.45 j/cm^2). The results presented in Figure 8 show that the composite exhibits attractive mechanical characteristics compared to a PVB film alone. Despite a drastic reduction in tensile stress, there is a strong increase in the elongation at break property, which is very important for resistance in the case of impact (Petroudy, 2017). In addition, there was a 13% increase of energy absorbed at break.

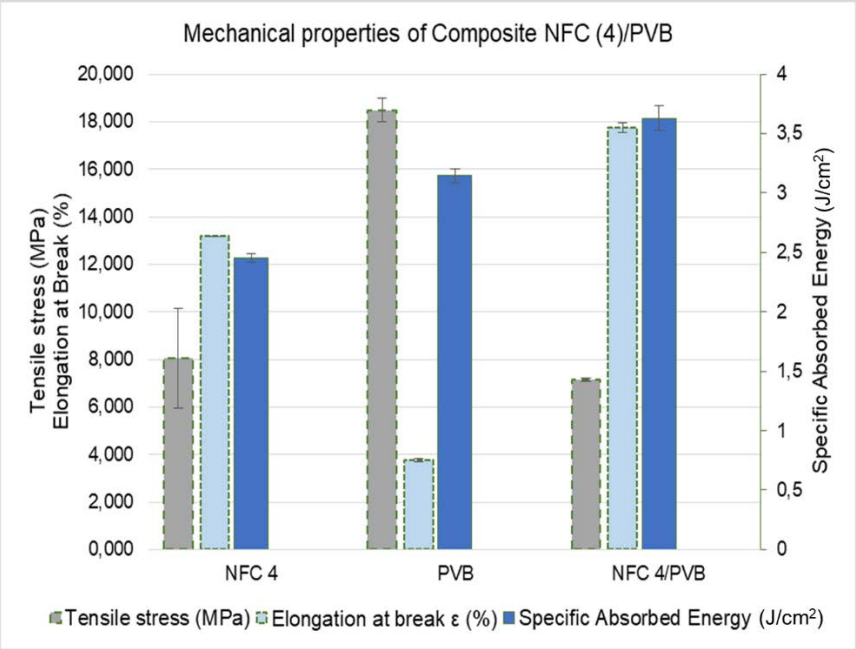

Figure 8.Mechanical properties of Composite NFC (4)/PVB

4. Conclusions

In the present study, different films were prepared by modifying the NFC oxidized TEMPO by different amounts of GMA and glycerol. The synthesized films have interesting properties such as transparency, flexibility, resistance and a less hydrophilic nature. The response surface methodology (RSM) was successfully applied to model and optimize the performance of modified NFC-based films. The optimal conditions for modification depend on the objectives. For example, to get the best flexibility independently of the other parameters, it is necessary to work with 2.25 ml of GMA and 0.5 ml of glycerol (NFC 9 Film). If we are looking for a good compromise between

flexibility, hydrophobicity, and transparency, NFC 5 is a good candidate with volumes of GMA and glycerol of 4.5 and 1 ml respectively. The enhancement of the properties can make these films a potential alternative to petroleum-based films depending on the target applications such as electronic substrates, cars, packaging, sports equipment, etc. It could also position this solution as candidates for interlayers in security glazing.

5. Acknowledgments

The authors are grateful for the financial support of the Mathematics of Information Technology and Complex Systems (MITACS NCE) and the Natural Sciences and Engineering Research Council of Canada (NSERC).

6. References

Abbasi, A., Nasef, M. M., Faridi-Majidi, R., Etesami, M., Takeshi, M., & Abouzari-Lotf, E. (2018). Highly flexible method for fabrication of poly (Glycidyl Methacrylate) grafted polyolefin nanofiber. Radiation Physics and Chemistry, 151, 283-291.

Abral, H., Ariksa, J., Mahardika, M., Handayani, D., Aminah, I., Sandrawati, N., Pratama, A., Fajri, N., Sapuan, S., Ilyas, R. (2020). Transparent and antimicrobial cellulose film from ginger nanofiber. Food Hydrocolloids, 98, 105266.

Ashori, A., Babaee, M., Jonoobi, M., & Hamzeh, Y. (2014). Solvent-free acetylation of cellulose nanofibers for improving compatibility and dispersion. Carbohydrate Polymers, 102, 369-375.

Bagheri, F., Radi, M., & Amiri, S. (2019). Drying conditions highly influence the characteristics of glycerol-plasticized alginate films. Food Hydrocolloids, 90, 162-171.

Bideau, B., Cherpozat, L., Loranger, E., & Daneault, C. (2016). Conductive nanocomposites based on TEMPO-oxidized cellulose and poly (N-3-aminopropylpyrrole-co-pyrrole). Industrial Crops and Products, 93, 136-141.

Cherifi, Z., Boukoussa, B., Zaoui, A., Belbachir, M., & Meghabar, R. (2018). Structural, morphological and thermal properties of nanocomposites poly (GMA)/clay prepared by ultrasound and in-situ polymerization. Ultrasonics Sonochemistry, 48, 188-198.

Coupland, J. N., Shaw, N. B., Monahan, F. J., O'Riordan, E. D., & O'Sullivan, M. (2000). Modeling the effect of glycerol on the moisture sorption behavior of whey protein edible films. Journal of Food Engineering, 43(1), 25-30.

Faria, M., Vilela, C., Mohammadkazemi, F., Silvestre, A. J., Freire, C. S., & Cordeiro, N. (2019). Poly (glycidyl methacrylate)/bacterial cellulose nanocomposites: Preparation, characterization and post-modification. International Journal of Biological Macromolecules, 127, 618-627.

Floyd, D. S. (2016). Plastic Oceans: A New Way in solving Our Plastic Pollution.

Fukuzumi, H., Saito, T., Iwata, T., Kumamoto, Y., & Isogai, A. (2009). Transparent and high gas barrier films of cellulose nanofibers prepared by TEMPO-Mediated oxidation. Biomacromolecules, 10(1), 162–165.

García, A., Gandini, A., Labidi, J., Belgacem, N., & Bras, J. (2016). Industrial and crop wastes: A new source for nanocellulose biorefinery. Industrial Crops and Products, 93, 26-38.

Huang, J., Zhong, Y., Zhang, L., Cai, J. (2017). Extremely Strong and Transparent Chitin Films: A High-Efficiency, Energy-Saving, and "Green" Route Using an Aqueous KOH/Urea Solution. Advanced Functional Materials, 27 (26) (2017).

Hild, F. (1992). De la rupture des matériaux à comportement fragile.

Islam, M. N., & Rahman, F. (2019). Production and modification of nanofibrillated cellulose composites and potential applications. In Green Composites for Automotive Applications (pp. 115-141): Elsevier

Khan, B. A., Na, H., Chevali, V., Warner, P., Zhu, J., & Wang, H. (2018). Glycidyl methacrylate-compatibilized poly (lactic acid)/hemp hurd biocomposites: Processing, crystallization, and thermo-mechanical response. Journal of Materials Science & Technology, 34(2), 387-397.

Kocak, G., Solmaz, G., Tuncer, C., & Bütün, V. (2019). Modification of glycidyl methacrylate based block copolymers and their aqueous solution behaviours. European Polymer Journal, 110, 364-377.

Kumar Singla, R., Maiti, S. N., & Ghosh, A. K. (2016). Crystallization, morphological, and mechanical response of poly (lactic acid)/lignin-based biodegradable composites. Polymer-Plastics Technology and Engineering, 55(5), 475-485.

Li, X., Zhang, H., He, L., Chen, Z., Tan, Z., You, R., & Wang, D. (2018). Flexible nanofibers-reinforced silk fibroin films plasticized by glycerol. Composites Part B: Engineering, 152, 305-310.

Liu, H., Adhikari, R., Guo, Q., & Adhikari, B. (2013). Preparation and characterization of glycerol plasticized (high-amylose) starch–chitosan films. Journal of Food Engineering, 116(2), 588-597.

Loranger, É., Paquin, M., Daneault, C., & Chabot, B. (2011). Comparative study of sonochemical effects in an ultrasonic bath and in a large-scale flow-through sonoreactor. Chemical Engineering Journal, 178, 359-365.

Loranger, É., Piché, A.-O., & Daneault, C. (2012). Influence of high shear dispersion on the production of cellulose nanofibers by ultrasound-assisted TEMPO-oxidation of kraft pulp. Nanomaterials, 2(3), 286-297.

Maury, C., Loranger, É., & Daneault, C. (2016). Development of nanocellulose-polyvinyl butyral composites for armored glass. SAMPE Conference Proceedings, Long Beach, California, USA, p.13.

Niu, Q., Gao, K., & Wu, W. (2014). Cellulose nanofibril based graft conjugated polymer films act as a chemosensor for nitroaromatic. Carbohydrate Polymers, 110, 47-52.

Paquin, M., Loranger, É., Hannaux, V., Chabot, B., & Daneault, C. (2013). The use of Weissler method for scale-up a Kraft pulp oxidation by TEMPO-mediated system from a batch mode to a continuous flow-through sonoreactor. Ultrasonics Sonochemistry, 20(1), 103-108.

Petroudy, S. D. (2017). Physical and mechanical properties of natural fibers. In Advanced High Strength Natural Fibre Composites in Construction (pp. 59-83): Elsevier

Pracella, M., Haque, M. M.-U., Paci, M., & Alvarez, V. (2016). Property tuning of poly (lactic acid)/cellulose bio-composites through blending with modified ethylene-vinyl acetate copolymer. Carbohydrate Polymers, 137, 515-524.

Rattaz, A., Mishra, S. P., Chabot, B., & Daneault, C. (2011). Cellulose nanofibres by sonocatalysed-TEMPO-oxidation. Cellulose, 18(3), 585.

Reis, A. V., Fajardo, A. R., Schuquel, I. T., Guilherme, M. R., Vidotti, G. J., Rubira, A. F., & Muniz, E. C. (2009). Reaction of glycidyl methacrylate at the hydroxyl and carboxylic groups of poly (vinyl alcohol) and poly (acrylic acid): is this reaction mechanism still unclear? The Journal of Organic Chemistry, 74(10), 3750-3757.

Rol, F., Belgacem, M. N., Gandini, A., & Bras, J. (2019). Recent advances in surface-modified cellulose nanofibrils. Progress in Polymer Science, 88, 241-264.

Simon, N., & Schulte, M. L. (2017). En finir avec la pollution plastique mondiale: les arguments en faveur d'une convention internationale. Repéré à https://ma.boell.org/sites/default/files/stopping_global_plastic_pollution_french_5final.pdf

Šoltýs, A., Hronský, V., Šmídová, N., Olčák, D., Ivanič, F., & Chodák, I. (2019). Solid-state 1H and 13C NMR of corn starch plasticized with glycerol and urea. European Polymer Journal, 117, 19-27.

Syverud, K., Xhanari, K., Chinga-Carrasco, G., Yu, Y., & Stenius, P. (2011). Films made of cellulose nanofibrils: surface modification by adsorption of a cationic surfactant and characterization by computer-assisted electron microscopy. Journal of Nanoparticle Research, 13(2), 773-782.

Tedeschi, G., Guzman-Puyol, S., Paul, U. C., Barthel, M. J., Goldoni, L., Caputo, G., Ceseracciu, L., Athanassiou, A., Heredia-Guerrero, J. A. (2018). Thermoplastic cellulose acetate oleate films with high barrier properties and ductile behaviour. Chemical Engineering Journal, 348, 840-849.

Tong, R., Chen, G., Tian, J., & He, M. (2020). Highly transparent, weakly hydrophilic and biodegradable cellulose film for flexible electroluminescent devices. Carbohydrate Polymers, 227, 115366.

Xhanari, K., Syverud, K., Chinga-Carrasco, G., Paso, K., & Stenius, P. (2011). Reduction of water wettability of nanofibrillated cellulose by adsorption of cationic surfactants. Cellulose, 18(2), 257-270.